Available online at www.sciencedirect.com
ScienceDirect
Journal of Power Sources 176 (2008) 347–352
JOURNAL OF POWER SOURCES
www.elsevier.com/locate/jpowsour

Short communication

Thermal stability of disordered carbon negative-electrode materials prepared from peanut shells

Izumi Watanabe [a], Takayuki Doi [a,*], Jun-ichi Yamaki [a], Y.Y. Lin [b], George Ting-Kuo Fey [b]

[a] *Institute for Materials Chemistry and Engineering, Kyushu University, 6-1 Kasuga-koen, Kasuga 816-8580, Japan*
[b] *Department of Chemistry & Material Engineering, National Central University, Chungli 32054, Taiwan, ROC*

Received 7 May 2007; received in revised form 30 October 2007; accepted 31 October 2007
Available online 6 November 2007

Abstract

The thermal stability of electrochemically lithiated disordered carbon with a poly(vinylidene difluoride) binder and 1 mol dm^{-3} $LiPF_6$ dissolved in a mixture of ethylene carbonate (EC) and diethyl carbonate (DEC) was investigated by differential scanning calorimetry (DSC) using a hermetically sealed pan. The disordered carbon used was prepared by pyrolyzing peanut shells with porogen at temperatures above 500 °C. The disordered carbon gave much larger charge and discharge capacities than graphite when a weight ratio of porogen to peanut shells was set at 5. In DSC curves, several exothermic peaks were observed at temperatures ranging from 120 to 310 °C. This behavior was similar to that for electrochemically lithiated graphite, except for an exothermic peak at around 250 °C. However, the lithiated disordered carbon had a higher heat value, which was evaluated by integrating a DSC curve, compared to lithiated graphite. The heat values increased with an increase in accumulated irreversible capacities. These results suggest that heat generation at elevated temperatures should increase as an amount of irreversibly trapped lithium-ion increases. On the other hand, heat values per reversible capacities for disordered carbon, which showed larger capacities than graphite, were almost comparable to that for graphite. These results indicate that several types of disordered carbon showed larger capacity than graphite, while their thermal stability was lowered accordingly.

Keywords: Lithium-ion battery; Thermal stability; Safety; Disordered carbon; Negative electrode

1. Introduction

Lithium-ion batteries have been extensively studied because of their high performance and potential. Due to their high energy densities, lithium-ion batteries have been considered as possible power sources in hybrid electric vehicles and electric vehicles. However, before lithium-ion batteries can be used in high-power applications, their performance still needs to improve in terms of battery cycle life, rate capability, and safety. The safety of lithium-ion batteries is closely related to the thermal stability of their constituent materials at elevated temperatures. Several exothermic reactions are known to occur in lithium-ion batteries at elevated temperatures [1]. If a safety vent on a cell can open to release high-pressure gas to the outside of lithium-ion batteries, a balance between heat evolution and thermal diffusion should be achieved even at high temperatures. On the other hand, it is generally accepted that "thermal runaway" could occur if heat evolution exceeds thermal diffusion. Thermal radiation waves are then sometimes visible as flames when constituent materials of lithium-ion batteries are heated to unusually high temperatures. A number of studies have been done to clarify the thermal runaway mechanism and/or to improve the thermal stability of lithium-ion batteries [2–12]. Some of them focused on the thermal stability of negative-electrode materials [3–12]. The thermal stability of a graphite negative-electrode in an electrolyte is controlled by solid electrolyte interphase (SEI) that is formed on the graphite electrode during initial charging [3,4,6,9,11]. Our group previously reported that SEI on lithiated graphite in EC + DMC-based electrolyte should break down thermally at around 280 °C [12]. In addition, the breakdown of SEI could be improved by 110 °C by using methyl difluoroacetate-based electrolyte compared to EC + DMC-based electrolyte [13]. Thus, there have been vast studies on the thermal stability of graphitic carbon electrodes.

* Corresponding author. Tel.: +81 92 583 7657; fax: +81 92 583 7791.
E-mail address: doi@cm.kyushu-u.ac.jp (T. Doi).

0378-7753/$ – see front matter © 2007 Elsevier B.V. All rights reserved.
doi:10.1016/j.jpowsour.2007.10.087

Various kinds of carbonaceous materials have been studied for use as a negative electrode in lithium-ion batteries [14]. Graphite, which shows an acceptably high capacity and a very flat potential close to lithium metal in charge/discharge processes, has been generally used for commercial applications [15]. However, other carbonaceous materials have also been studied as alternatives to enhance the performance of lithium-ion batteries. Among them, some types of non-graphitizable carbon show relatively higher capacity than graphite, which makes non-graphitizable carbon a possible candidate for use as a negative electrode in lithium-ion batteries for hybrid electric vehicles [16–25]. Non-graphitizable carbon shows different electrochemical properties depending on the nature of the precursor. Dahn et al. studied the electrochemical behavior of some types of non-graphitizable carbon in a liquid electrolyte, and reported that they showed higher reversible capacity than graphitic carbon (~372 mA h g^{-1}) [16]. A lithium-ion insertion and extraction mechanism at a non-graphitizable carbon electrode has also been reported [19–24]. However, little attention has been paid to the thermal stability of non-graphitizable carbon electrode. In this work, the thermal stability of a disordered carbon electrode with EC + DMC-based electrolyte containing $LiPF_6$ was investigated by DSC.

2. Experimental

Disordered carbon was prepared by pyrolyzing peanut shells with proprietary porogenic agents at temperatures between 500 and 800 °C. A weight ratio of porogen to peanut shells was set at from 1 to 5. The preparation method has been described in detail previously [18]. The composition of the product materials was investigated by an elemental analyzer (CHN 2000, PerkinElmer Inc.).

Disordered carbon used here is hereafter referred to as C-1-500, C-3-500, C-5-500, C-5-700, and C-5-800; where the numbers to the right of "C-" represent the weight ratio of porogen/peanut shells and preparation temperature.

The electrochemical properties of the resultant disordered carbon were investigated by charge and discharge measurements (BTS-2004W, Nagano Co. Ltd.) using a coin cell. The working electrode was prepared by coating a slurry of the resultant disordered carbon and poly(vinylidene difluoride) (PVdF) in *N*-methyl-2-pyrrolidone on copper foil. The weight ratio of PVdF to disordered carbon was set at 5/95 for C-1-500 and C-3-500, and 14/86 for C-5-500, C-5-700, and C-5-800. The electrodes were then dried for 12 h at 70 °C in a vacuum oven, which was about 100 μm thick. A coin cell was assembled using a disordered carbon electrode of 15 mm in diameter, a Li foil of 15 mm in diameter as a counter electrode, a polypropylene separator (Celgard 3501), and a liquid electrolyte of 1 mol dm^{-3} $LiPF_6$ dissolved in EC + DMC (1:1 by volume, Tomiyama Pure chemical Industries Ltd.). The cell was cycled between 0.01 and 3 V at a constant current rate of 0.2 mA cm^{-2} with a relaxation period of 60 min at the end of discharging.

After the 5th cycle, a cell was charged to 0.01 V to obtain a charged disordered carbon electrode. The cell was then disassembled in an Ar-filled glove box to take it out. About 5 mg of the electrode containing some amount of electrolyte was packed in a hermetically sealed pan made of stainless 304. The thermal stability was investigated by DSC combined with thermogravimetric analysis (Thermo plus TG8110, Rigaku Corp.) at a heating rate of 5 °C min^{-1} from room temperature to 400 °C. No leakage occurred during measurements, which was confirmed by the absence of weight loss in TG curves that had been obtained concurrently with DSC. All experiments were conducted under an Ar atmosphere with a dew point below −70 °C.

3. Results and discussion

Fig. 1 shows H/C ratios of resultant carbonaceous materials. The carbonaceous materials prepared at 500 °C had H/C ratios of about 0.25 regardless of the weight ratio of porogen to peanut shells. The H/C ratio gradually decreased with an increase in reaction temperature: C-5-700 and C-5-800 exhibited 0.14 and 0.10, respectively. These values were consistently less than those reported in previous work even though the carbonaceous materials were prepared in the same way [18]. These differences are probably due to the dehydrogenation and/or dehydration of the carbonaceous materials upon storage; remnants of the porogen may abstract hydrogen from the carbonaceous materials (dehydrogenation).

Fig. 2 shows the charge and discharge characteristics at the 1st, 2nd, and 10th cycles of C-5-800. A large divergence between insertion and extraction potentials, which is commonly referred to as hysteresis, was seen and could be attributed to the high H/C ratio above 0.1 [25]. A very large capacity of 2260 mA h g^{-1} was obtained during the initial charge. However, the irreversible capacity in the initial cycle, which was evaluated to 1395 mA h g^{-1}, was also very large. This is likely due to trapped lithium-ions within nano-sized pores of the carbonaceous materials, irreversible reactions of lithium-ions with

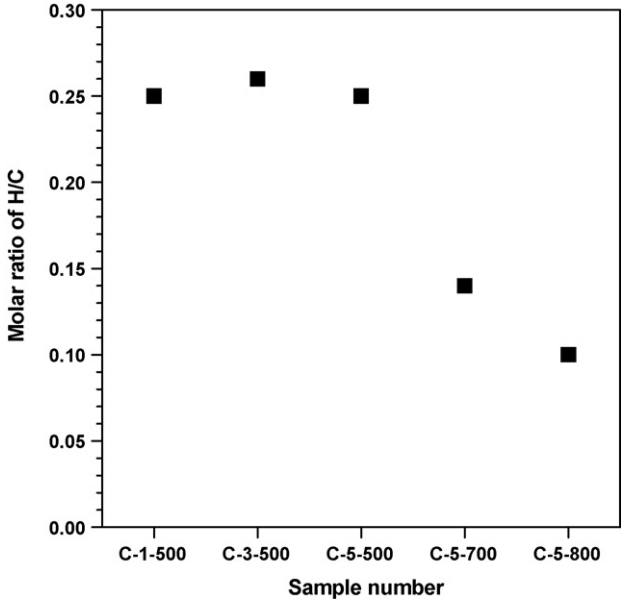

Fig. 1. H/C ratios of C-1-500, C-3-500, C-5-500, C-5-700, and C-5-800.

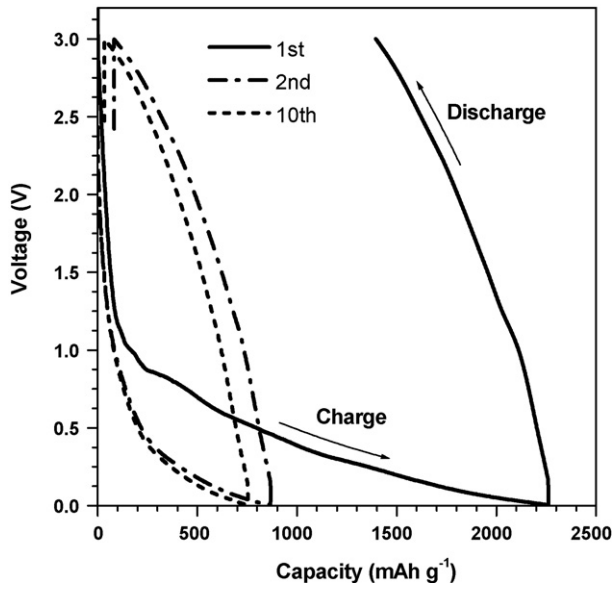

Fig. 2. Charge and discharge curves of C-5-800 in 1 mol dm^{-3} $LiPF_6$ dissolved in EC + DMC at the 1st, 2nd, and 10th cycles.

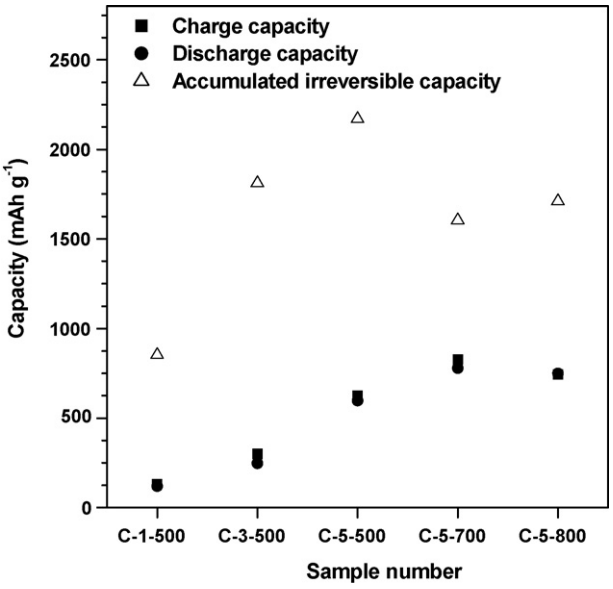

Fig. 4. Charge and discharge capacities at the 5th cycle, and accumulated irreversible capacities from the 1st to 5th cycles for C-1-500, C-3-500, C-5-500, C-5-700, and C-5-800.

surface functional groups such as hydroxyls and carboxyls, and/or formation of the surface film on the electrode [26,27]. The irreversible capacity significantly decreased after the 2nd cycle and the reversible capacity of around 700 mA h g^{-1} was obtained even after the 10th cycle, as shown in Fig. 2. Almost identical tendencies were observed in the charge and discharge curves for C-1-500, C-3-500, C-5-500, and C-5-700. Fig. 3 shows variation of charge and discharge capacities with cycle number for C-5-800, together with the Coulombic efficiency of it. Irreversible capacities gradually decreased with increasing cycle number after the 2nd cycle. Charge/discharge efficiency reached more than 95% after the 5th cycle. The reversible capacity was still 667 mA h g^{-1} at the 25th cycle.

Fig. 4 shows charge and discharge capacities at the 5th cycle, and accumulated irreversible capacities from the 1st to 5th cycles for C-1-500, C-3-500, C-5-500, C-5-700, and C-5-800. C-1-500, C-3-500, and C-5-500 gave reversible capacities of 119, 247, and 598 mA h g^{-1}, and irreversible capacities of 853, 1811, and 2170 mA h g^{-1}, respectively. These results indicate that the charge and discharge capacities for the carbonaceous materials prepared at 500 °C increased as the ratio of porogen to peanut shells increased. The H/C ratio remained unchanged at around 0.25 regardless of the porogen/peanut shells ratio at 500 °C, as shown in Fig. 1. On the other hand, the number of nano-sized pores in resultant carbonaceous materials should increase proportionally with the porogen/peanut shells ratio [18]. Some of the pores would accommodate and release lithium-ions reversibly, but others trap them irreversibly [28–31]. Hence, both the reversible and the irreversible capacities increased with an increase in a porogen/peanut shells ratio in this work. Another mechanism involves the carbonization of peanut shells containing porogen during heat treatment up to 500 °C. The decomposition of porogen should be accompanied by exothermic heat, which is likely to promote the organization of carbonaceous materials. In fact, in XRD patterns shown in Ref. [18], diffraction peaks at around 26 and 43° in 2θ of carbonaceous materials became more noticeable with an increase in a porogen/peanut shells ratio. These results suggest that the resultant carbonaceous materials should be crystallized with an increase in a porogen/peanut shells ratio, which seems to lead to an increase in the discharge capacities as well as the charge capacities. C-5-700 and C-5-800 exhibited much larger discharge and charge capacities than C-5-500. In particular, the largest values of reversible (779 mA h g^{-1}) and irreversible capacities (828 mA h g^{-1}) were obtained for C-5-700 in this work. In addition, C-5-700 gave the smallest value of accumulated irreversible capacity of 1510 mA h g^{-1}.

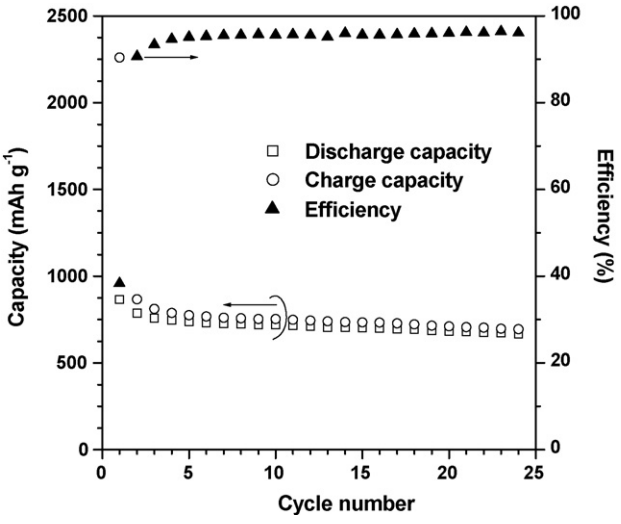

Fig. 3. Variation of charge and discharge capacity with cycle number for C-5-800 electrode, together with the Coulombic efficiency of it.

Fig. 5 shows DSC curves of fully lithiated C-1-500, C-3-500, C-5-500, C-5-700, and C-5-800. The heat flow is based on the

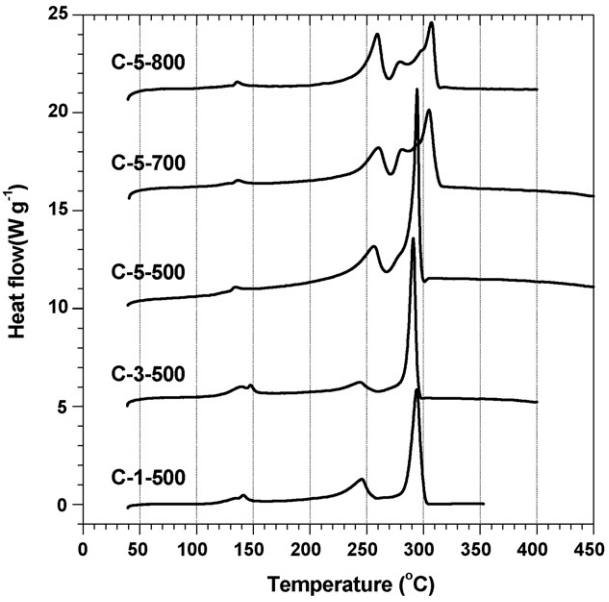

Fig. 5. DSC curves of fully lithiated C-1-500, C-3-500, C-5-500, C-5-700, and C-5-800 *i*th 1 mol dm^{-3} $LiPF_6$/EC + DMC.

total weight of the sample. All the DSC curves in Fig. 5 showed mild heat generation starting from about 120 °C with a small exothermic peak at around 140 °C. Almost the same behavior was observed for lithiated graphite electrode [12]. Based on discussion in the literature, the small peak at 140 °C seems to be caused by the reaction between the electrolyte and lithiated graphite where the surface is not covered with SEI but with PVdF-binder. Since the binder should be swollen by an electrolyte at elevated temperatures, surface film seems to be newly formed on the carbon surface that had been covered with the binder [12]. In addition, the exothermic peak at 140 °C is also likely due to conversion of surface film into a more stable one and/or further growth of surface film accompanied by electrolyte decomposition [6].

Mild heat generation occurred from about 120 °C and it continued until a broad exothermic peak appeared at around 250 °C for all the DSC curves. Similar continuous heat generation was also seen for a lithiated graphite electrode in our previous work [12]. Based on the results, it is likely due to a heterogeneous reaction in which an electrolyte permeates through the existing surface film onto the lithiated carbon surface to form a new surface film. A significant amount of heat generation occurred at temperatures ranging from 270 to 310 °C for all the DSC curves in Fig. 5. A very sharp exothermic peak was observed at around 295 °C for C-1-500, C-3-500, and C-5-500, together with a small shoulder peak at about 280 °C. The shoulder peak became more significant with an increase in a porogen/peanut shells ratio, and was more obvious for C-5-700 and C-5-800. In contrast to a sharp peak at about 295 °C for the carbonaceous materials prepared at 500 °C, the corresponding peak appeared as two peaks for C-5-700 and C-5-800; a sharp peak at about 305 °C with a small shoulder peak at around 295 °C was observed. Our group previously showed that lithiated graphite gave a very sharp peak at temperatures ranging from 270 to 310 °C, which is due to a direct reaction between lithiated graphite and the electrolyte accompanied by a breakdown of SEI [12]. On the other hand, three exothermic peaks appeared around 300 °C for C-5-700 and C-5-800, as described above. The structure of the crystallites in disordered carbon is known to be crystallized with an increase in preparation temperature. In addition, several types of disordered carbon show higher reversible capacities than graphitic carbon. Several models have been proposed to explain these high specific capacities, including lithium storage in nano-sized pores and adsorption of lithium-ion on both sides of a single graphite-like sheet [20,21]. Based on the findings that the charge and discharge characteristics for C-5-700 and C-5-800 were different from C-5-500, the structure and/or crystallinity of disordered carbon should be significantly developed at around 700 °C. In other words, several kinds of reversible insertion sites for lithium-ion with different energy states are likely to be formed at temperatures above 700 °C. Accordingly, C-5-700 and C-5-800 would show the multiple peaks around 300 °C in DSC curves depending on chemical potentials of inserted lithium-ion within disordered carbon. On the other hand, the exothermic peak at around 250 °C was characteristic of lithiated disordered carbon since it was not observed for the lithiated graphite. There is an obvious difference in charge and discharge characteristics between graphitic carbon and disordered carbon electrodes; a considerable amount of lithium-ion is known to be trapped within the disordered carbon, as shown in Fig. 2. Since the amount of heat generation at around 250 °C tended to increase with accumulated irreversible capacities from the 1st to the 5th cycle, such trapped lithium-ion may be activated at elevated temperatures to react with an electrolyte at around 250 °C.

The total amount of heat generation was evaluated by integrating the DSC curves shown in Fig. 5: C-1-500, C-3-500, C-5-500, C-5-700, and C-5-800 gave 1499, 1566, 2050, 2085,

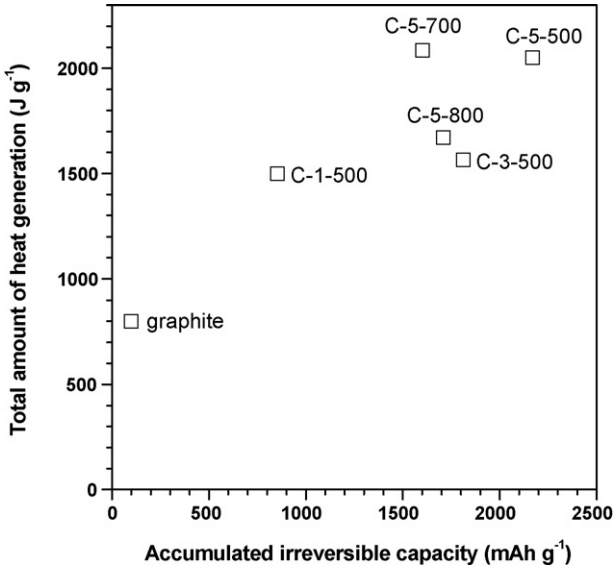

Fig. 6. Total amount of heat generation against accumulated irreversible capacities from the 1st to 5th cycle for C-1-500, C-3-500, C-5-500, C-5-700, and C-5-800, together with that for a fully lithiated graphite derived from Ref. [12]. The total amount of heat generation was evaluated from DSC curves in Fig. 5.

and 1671 J g^{-1}, respectively. At a preparation temperature of 500 °C, the total amount of heat generation increased with an increasing ratio of porogen to peanut shells. The largest value was obtained for C-5-700. The heat values against accumulated irreversible capacities from the 1st to 5th cycle are shown in Fig. 6, together with that for lithiated graphite obtained in previous work [12]. The lithiated graphite generated much smaller heat of 800 J g^{-1} than lithiated disordered carbon used in this work. Total amount of heat generation increased with an increase of accumulated irreversible capacities, as is evident from Fig. 6. These results indicate that heat generation should increase depending on the amount of irreversibly consumed lithium-ion; active lithium-ion was consumed by irreversible reactions with surface functional groups such as hydroxyls and carboxyls, formation of the surface film on the electrode, and/or being trapped within nano-sized pores in disordered carbon. Among them, lithium-ion trapped within the disordered carbon should be very reactive, in particular, at elevated temperatures. Hence, such lithium-ion seems to be mainly related to the heat generation though the detailed mechanism of the exothermic reactions is not yet clear. More quantitative discussion would be possible if we can evaluate the amount of trapped lithium-ions. The heat generation at elevated temperatures should be suppressed to enhance the safety of lithium-ion batteries. The disordered carbon used here seems to possess lower thermal stability as active materials in the batteries than graphitic carbon. Therefore, an irreversible capacity should be reduced to enhance thermal stability of a disordered carbon electrode. The heat values and the heat values per reversible capacities at the 5th cycle versus reversible capacities are shown in Fig. 7a and b, respectively, together with that for lithiated graphite obtained in previous work [12]. C-1-500 and C-3-500, which gave smaller reversible capacities than graphite, exhibited 12.6 and 6.3 J mA h^{-1}, respectively. These values are much larger than 2.7 J mA h^{-1} for graphite. On the other hand, C-5-500, C-5-700, and C-5-800, which showed larger capacities than graphite, gave 3.4, 2.7, and 2.2 J mA h^{-1}, respectively. These values are almost comparable to that for graphite. Based on the present results, several types of disordered carbon showed larger capacity than graphite, while their thermal stability lowered accordingly.

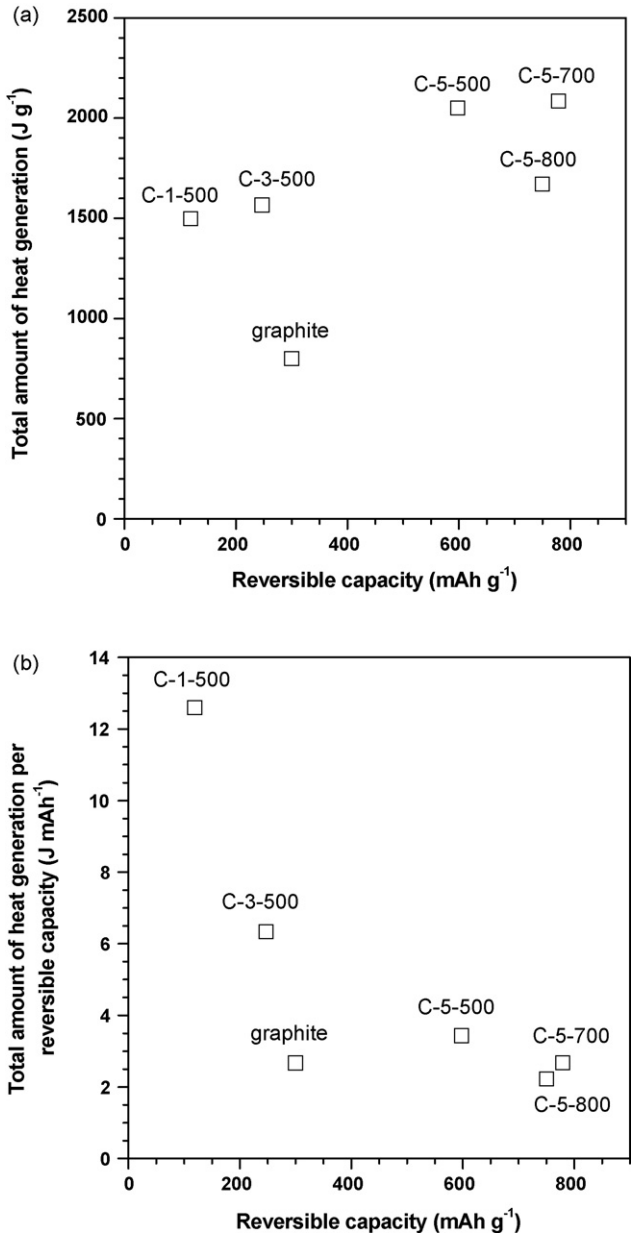

Fig. 7. (a) Heat values and (b) the heat values per reversible capacities at the 5th cycle against the reversible capacities.

4. Conclusion

Thermal stability of lithiated disordered carbon was investigated by DSC. The disordered carbon was prepared by pyrolyzing peanut shells containing porogen at temperatures above 500 °C. Although a large hysteresis in voltage was seen during charge and discharge, C-5-500, C-5-700, and C-5-800 exhibited higher charge and discharge capacities than graphite. The DSC curves showed mild heat generation that started from about 120 °C with a small exothermic peak at around 140 °C. In addition, a broad exothermic peak appeared at around 250 °C, which was characteristic of lithiated disordered carbon. A significant amount of heat generation was observed at temperatures ranging from 270 to 310 °C, which is due to a direct reaction between lithiated disordered carbon and electrolyte accompanied by a breakdown of the surface film. The total amount of heat generation were much larger than those obtained for lithiated graphite in the previous work. In addition, the total amount of heat generation tended to increase with an increase in accumulated irreversible capacities. These results suggest that heat generation at elevated temperatures should increase as the amount of irreversibly trapped lithium-ion increases. Therefore, an irreversible capacity should be reduced to enhance the thermal stability of a disordered carbon electrode in lithium-ion batteries. On the other hand, the heat values per reversible capacities for C-5-500, C-5-700, and C-5-800, which showed larger capacities than graphite, were almost comparable to that for graphite. Although several types of disordered carbon possessed larger capacity than graphite, their thermal stability lowered accordingly.

Acknowledgement

The present work was supported by CREST (Core Research for Evolutional Science and Technology) of JST (Japan Science and Technology Agency).

References

[1] U. von Sacken, J.R. Dahn, Extended Abstracts of Electrochemical Society Fall Meeting, vol. 54, 1990, p. 87.
[2] S. Tobishima, J. Yamaki, J. Power Sources 81/82 (1999) 882.
[3] U. von Sacken, E. Nodwell, A. Sundher, J.R. Dahn, J. Power Sources 54 (1995) 240.
[4] Z. Zhang, D. Fouchard, J.R. Rea, J. Power Sources 70 (1998) 16.
[5] A. Du Pasquier, F. Disma, T. Bowmer, A.S. Gozdz, G. Amatucci, J.-M. Tarascon, J. Electrochem. Soc. 145 (1998) 472.
[6] M.N. Richard, J.R. Dahn, J. Electrochem. Soc. 146 (1999) 2068.
[7] M.N. Richard, J.R. Dahn, J. Electrochem. Soc. 146 (1999) 2078.
[8] D.D. MacNeil, D. Larcher, J.R. Dahn, J. Electrochem. Soc. 146 (1999) 3596.
[9] A.M. Andersson, K. Edstrom, J.O. Thomas, J. Power Sources 81/82 (1999) 8.
[10] A. Okamoto, T. Sasaki, S. Komatsu, K. Nakamitsu, H. Tsukamoto, M. Mizutani, GS News Tech. Rep. 56 (1999) 18.
[11] K. Edstrom, A.M. Andersson, A. Bishop, L. Fransson, J. Lindgren, A. Hussenius, J. Power Sources 97/98 (2001) 87.
[12] J. Yamaki, H. Takatsuji, T. Kawamura, M. Egashira, Solid State Ionics 148 (2002) 241.
[13] M. Ihara, B.T. Hang, K. Sato, M. Egashira, S. Okada, J. Yamaki, J. Electrochem. Soc. 150 (2003) A1476.
[14] M. Winter, J.O. Besenhard, M.E. Spahr, P. Novák, Adv. Mater. 10 (1998) 725.
[15] Z. Ogumi, M. Inaba, Bull. Chem. Soc. Jpn. 71 (1998) 521.
[16] J.R. Dahn, T. Zheng, Y.H. Liu, J.S. Xue, Science 270 (1995) 590.
[17] T. Iijima, K. Suzuki, Y. Matsuda, Synth. Metals 73 (1995) 9.
[18] G.T.K. Fey, D.C. Lee, Y.Y. Lin, T.P. Kumar, Synth. Metals 139 (2003) 71.
[19] K. Sato, M. Noguchi, A. Demachi, N. Oki, M. Endo, Science 264 (1994) 556.
[20] A. Mabuchi, K. Tokumitsu, H. Fujimoto, T. Kasuh, J. Electrochem. Soc. 142 (1995) 1041.
[21] J.S. Xue, J.R. Dahn, J. Electrochem. Soc. 142 (1995) 3668.
[22] T. Doi, K. Miyatake, Y. Iriyama, T. Abe, Z. Ogumi, T. Nishizawa, Carbon 42 (2004) 3183.
[23] T. Doi, Y. Iriyama, T. Abe, Z. Ogumi, J. Electrochem. Soc. 152 (2005) A1521.
[24] T. Doi, Y. Iriyama, T. Abe, Z. Ogumi, J. Power Sources 142 (2005) 329.
[25] T. Zheng, J.S. Xue, J.R. Dahn, Chem. Mater. 8 (1996) 389.
[26] K. Guerina, A. Fevrier-Bouviera, S. Flandrois, B. Simonb, P. Biensan, Electrochim. Acta 45 (2000) 1607.
[27] W. Xing, J.R. Dahn, J. Electrochem. Soc. 144 (1997) 1195.
[28] A. Mabuchi, K. Tokumitsu, H. Fujimoto, T. Kasuh, J. Electrochem. Soc. 142 (1995) 104.
[29] E. Buiel, A.E. George, J.R. Dahn, J. Electrochem. Soc. 145 (1998) 2252.
[30] K. Tatsumi, J. Conard, M. Nakahara, S. Menu, P. Lauginie, Y. Sawada, Z. Ogumi, J. Electrochem. Soc. 145 (1998) 2252.
[31] M. Nagao, C. Pitteloud, T. Kamiyama, T. Otomo, K. Itoh, T. Fukunaga, K. Tatsumi, R. Kanno, J. Electrochem. Soc. 153 (2006) A914.